2E2-1

Evaluation of the UWB Transmission Model by Using Frequency-Domain Near-Field to Near-Field Transformation Applied to the Parallel Computing

Ken-ichi Asanuma [1], Tadahiko Maeda [1]
[1] Graduate School of Science and Engineering at Ritsumeikan University

1. Introduction

To assess the actual performance of UWB transmission systems, various relative angles between the transmitting antenna and receiving antenna must been evaluated, considering the actual relative positions of mobile terminals. In the case of far-field conditions, the transmission model can be described using the angular characteristics of the antenna transfer functions [1]. In contrast, in the case of near-field conditions, 3D-conformal FDTD technique [2] or high-resolution staircase approximation can be generally used to obtain accurate results for the skewed models where the transmitting and receiving antennas are not placed in parallel. However, these two solutions take significant calculation time because the analytical models should be prepared as a parameter of the angle between both antennas. Therefore, the MRFDTD (Multi-Region FDTD) method, which incorporates the separated multi-analytical region using near-field to near-field transformation (NFNFTF) as one of the more convenient solutions, was reported in [3]. While several studies and results with NFNFTF based on the time-domain implementation [4][5] have been reported, time-domain NFNFTF in practice has some problems. For example, the waveform interpolation [5] and the random memory access caused by the time-shift from the source point to the observation point is not appropriate for parallel computing. In this paper, the MR-FDTD method using frequency-domain NFNFTF will be discussed.

2. MR-FDTD Method Using Frequency-domain NF-NF Transformation

Figure.1 shows the entire calculation flow. The goal of this paper is to evaluate the near-field UWB transmission characteristics for the various relative angles between transmitter and receiver. It is important to evaluate the waveform distortion caused by the skewed antenna geometry. Therefore, only one-way coupling (Tx -> Rx) between them will be calculated. (Calculation for the opposite direction is not required.) We evaluate the accuracy and computational efficiency for the incident fields using the following two formulas [6]:

Stratton-Chu Formula **(based on the spatial derivative at the source point):**

$$\bar{E}(\bar{r}) = \oiint_S \left[j\omega\mu \bar{J}(\bar{r}')\, g(\bar{r},\bar{r}') + \frac{1}{j\omega\varepsilon}\left(\nabla'\cdot\bar{J}(\bar{r}')\right)\nabla' g(\bar{r},\bar{r}') - \bar{J}_m(\bar{r}')\times\nabla' g(\bar{r},\bar{r}') \right] dS' \qquad (1)$$

Franz Formula **(based on the spatial derivative at the observation point):**

$$\bar{E}(\bar{r}) = \nabla\times\bar{A}, \qquad \bar{A} = \oiint_S \left[-\bar{J}_m(\bar{r}')\, g(\bar{r},\bar{r}') + \frac{j}{\omega\varepsilon}\bar{J}(\bar{r}')\times\nabla' g(\bar{r},\bar{r}') \right] dS' \qquad (2)$$

where $\bar{r}$ denotes the observation point, $\bar{r}'$ denotes the source point, g is the green's function in freespace, and J and J_m are the equivalent currents on the closed surface S. In the transmitter's region, these equivalent currents are calculated by real-time DFT and stored as data after completion of the simulation. Next, the incident fields are calculated by NFNFTF and converted to the time-domain waveform. Finally, the scattered fields $\bar{E}^s$ are obtained using the scattered field FDTD formulation as follows:

$$\bar{E}^{s,n} = \frac{2\varepsilon-\sigma\Delta t}{2\varepsilon+\sigma\Delta t}\bar{E}^{s,n-1} + \frac{2\Delta t}{2\varepsilon+\sigma\Delta t}\left(\nabla\times\bar{H}^{s,n-1/2} - \sigma\bar{E}^{i,n-1/2} - (\varepsilon-\varepsilon_0)\frac{\partial\bar{E}^{i,n-1/2}}{\partial t} \right) \qquad (3)$$

where σ is conductivity.

ISBN: 978-4-88552-223-9 C3055©IEICE

3. Calculated Results

3.1 Simulation Conditions

Figure.2 and 3 show the analytical model and coordinate system, respectively. In this section, we evaluate the near-field UWB transmission characteristics using CDA and CSA as the test antennas. The following three types of calculations were performed for both antennas: 1) Direct solution, 2) MRFDTD with Stratton formula, 3) MRFDTD with Franz formula. The MRFDTD model uses a uniform space lattice composed of 120×120×120cubic Yee cells (in the case of the direct solution: 270×120×120) having Δ=1mm, which is surrounded by an 8-layer PML. Each simulation is performed for 2000 time steps to ensure the Courant stability condition. In the case of MRFDTD, the incident fields were calculated in parallel using real-time 100-point DFT and IDFT over the frequency range from 0.5 to 14GHz in parallel. The excitation for the transmitting antenna was a fifth derivative Gaussian pulse of the form in (4):

$$v_g(t) = \frac{1}{\tau}\frac{d^5}{dt^5}\exp\left(-\left(\frac{4(t-\tau)}{\tau}\right)^2\right) - Ri(t) \tag{4}$$

with τ=3.1×10^{-10}, where $i(t)$ is the current at the feed point and R is the characteristic impedance of the feed line. We choose R=100Ω for CDA and R=250Ω for CSA. Finally, each computation was executed on four parallel-processors of the supercomputer system SX-7 at the Information Synergy Center, Tohoku University.

3.2 Efficiency Analysis of Each Solution

Table.1 summarizes the computing efficiencies obtained with the three different solutions: 1) Direct, 2) Stratton, and 3) Franz. First, Stratton-Chu formula solution is faster than the Franz formula solution. Second, the direct solution is the most efficient. However, the direct solution has some problems when evaluating the variations transmission characteristics as a parameter of the angle between both antennas: for example, 1) the analytical models should be prepared for the various configurations in terms of the relative angles between the Tx and Rx antennas, and 2) the size of the unit cell needs to be scaled down to 1/p in order to model the skew conditions with fine resolution. Therefore, in such cases, the direct solution takes expensive $O(p^4)$ operations (The estimated order of operations corresponds to the maximum possible computational load).

In contrast, MRFDTD solutions resolve these problems by the vector transformation of the incident fields in any skew conditions; thus, only $O(p)$ operations are assumed to be required. Moreover, the calculation of the surface current needs to be calculated once.

3.3 Computation Accuracy of the Incident Field

In this section, to evaluate the accuracy of the incident fields with three solutions, the spectrum of the dominant E-field component (E_θ for CDA, E_φ for CSA) at the two typical observation points of (θ, φ, d)=(90, 0, 75) and (θ, φ, d)=(90, 0, 150) are calculated as examples. Figure.4 and 5 show the calculated results. A relatively good agreement can be seen among the three solutions for the entire frequency range corresponding to the bandwidth of the applied DFT. However, the result obtained with the Franz formula is as much as 6dB below the result obtained with the direct solution seen at 9.3GHz in Fig.6, whereas the result obtained with Stratton-Chu formula is very close to the direct-computed incident fields. The diffracted waves from the edges of the conducting ground plane of CSA complicate the near-field E-field distribution; therefore, the solution with Stratton-Chu formula solution is more accurate because the spatial derivative of the fields is taken at the source point before the integration.

3.4 Simulation Example of Near-Field UWB Transmission Characteristics

The final example involves the received pulse and S_{21} of the near-field UWB transmission characteristics from CDA to CDA at (θ, φ, d) = (90, 0, 150). Figure.6 and 7 show the calculated results. In Fig.6, good agreement exists at the first peak of the received pulse. However, in the direct solution, the received pulse seems to include the mutual-coupling effect seen from the second peak at 2 nsec. This delayed wave includes the higher frequency components compared with the

first peak at 1 nsec; therefore, the mutual coupling effect appears mainly upper frequency band above the center frequency of the spectrum of this pulse. This phenomenon is demonstrated in Fig.7. Finally, the cross-correlation between the direct-computed pulse and the MRFDTD-computed pulse was evaluated under the various conditions by changing the azimuth angle. As a result, the angular characteristics of the cross-correlation were achieved over 0.98. Consequently, the mutual coupling effect can be ignored for the evaluation of near-field UWB transmission characteristics. Thus, MRFDTD method based on the frequency-domain NFNFTF has the advantages of being applicable parallel computing to reduce calculation costs.

4. Conclusion

In this paper, to evaluate the near-field UWB transmission characteristics for various relative angles between transmitting antenna and receiving antenna, we investigated the MRFDTD method based on the frequency-domain NFNFTF. First, we evaluated the computational efficiency and accuracy of the incident field with the three solutions: 1) Direct, 2) Stratton-Chu formula, and 3) Franz formula. Due to the excellent agreement between 1) and 2), we decided to use the Stratton-Chu formula. Next, we evaluated the near-field UWB transmission characteristics in both time-domain and frequency-domain. As the results show good agreement exists between the direct solution and the MRFDTD method with the Stratton-Chu formula. The results support the conclusion that frequency-domain NFNFTF can provide good agreement in terms of the evaluation of waveform distortion, even for various relative angles between antennas, without calculating the mutual coupling effect.

Acknowledgments

A part of this study was conducted under the auspices of a Grant-in-Aid for Scientific Research (basic research (B) 18300023) of the Japan Society for the Promotion of Science. This study also received assistance from 'Combined Large-scale Sensor System for Disaster Prevention and Safety and the Establishment of robust Network' of the High-tech Research Center Improvement Project for the Advancement of Academic Research in a Private University by the Ministry of Education, Culture, Sports, Science and Technology. Finally, a portion of the experimental results in this research was obtained using supercomputing resources at the Information Synergy Center, Tohoku University.

References

[1] K. Asanuma, D. Ushirogouchi, S. Yamamoto, T. Maeda, "Eigenvalue Distribution of the Multi-Element UWB Antenna Systems Including the Effects of Human Body," IEICE Technical Report AP2006-107, pp. 63-68, December 2006.

[2] S. Dey and R. Mittra, "A locally conformal finite-difference time-domain(FDTD) algorithm for modelling three-dimensional perfectly conducting objects," IEEE Microwave Guided Wave Lett., vol.7, pp.273-275, Sept.1997.

[3] A.Laisne, R.Gillard and G. Piton, "A new multiresolution near-field to near-field transform suitable for multi-region FDTD schemes," IEEE MTT-S International Microwave Symposium Digest, Volume 2, pp.893 -896, May 2001.

[4] K.L.Shlager and G.S. Smith, "Near-field to near-field transformation for use with FDTD method and its application to pulsed antenna problems," Electronics Letters, Volume 30, Issue 16, 4, pp.1262 - 1264, Aug. 1994.

[5] J. De Moerloose and D. De Zutter, "Surface integral representation radiation boundary condition for the FDTD method," IEEE Trans. on A.P., Volume 41, Issue 7, pp.890 - 896, July 1993.

[6] Chen-To Tai, "Kirchhoff theory: Scalar, vector, or dyadic?," IEEE Transactions on Antennas and Propagation, Volume 20, Issue 1, pp.114 - 115 , Jan 1972.

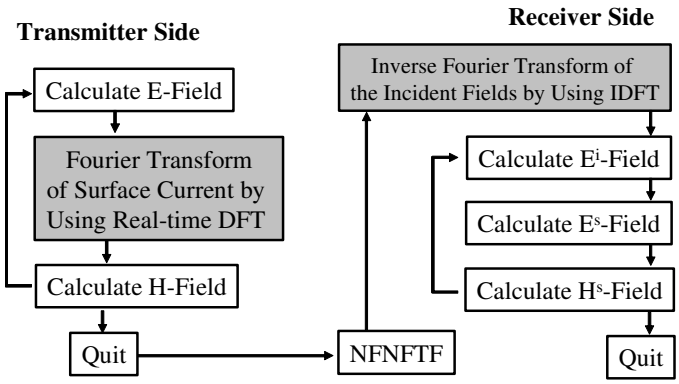

Figure 1: Calculation flow.

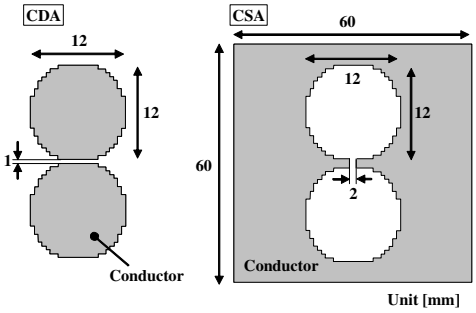

Figure 2: Analytical model.

Table1: Computing efficiency v.s. solutions.

Solutions	Time [sec]	Memory size [MB]	R_v[%]
Direct	253	768	98.4
Stratton	Tx: 307 Rx: 302	Tx: 576 Rx: 640	97.0 97.3
Franz	Tx: 307 Rx: 383	Tx: 576 Rx: 640	97.0 97.5

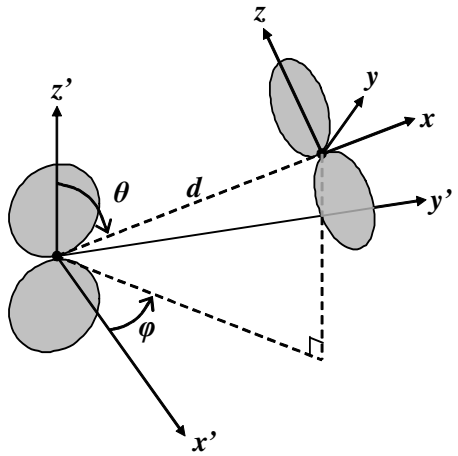

Figure 3: Coordinate system.

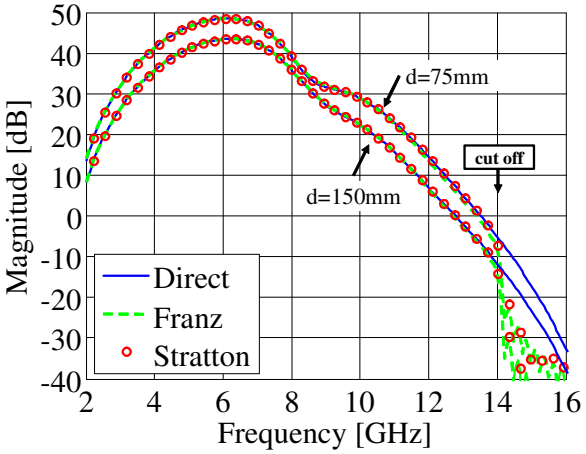

Figure 4: E-field spectrum (CDA).

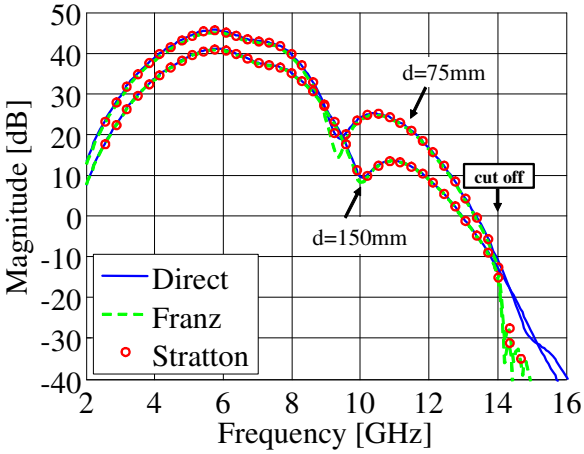

Figure 5: E-field spectrum (CSA).

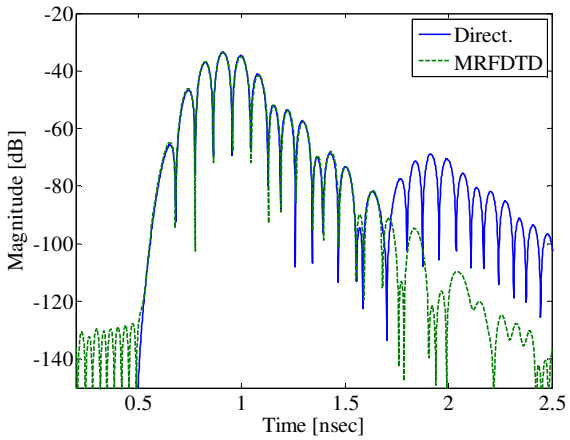

Figure 6: Received pulse (CDA)

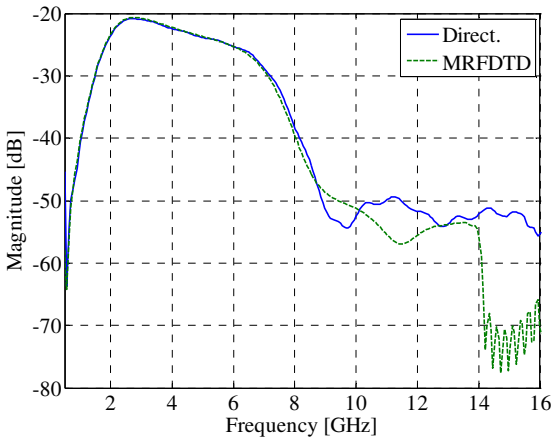

Figure 7: Magnitude of the transmission characteristics (CDA) .